Systems & Control Transactions

Research Article - Peer Reviewed Conference Proceeding
ESCAPE 35 - European Symposium on Computer Aided Process Engineering
Ghent, Belgium. 6-9 July 2025
Jan F.M. Van Impe, Grégoire Léonard, Satyajeet S. Bhonsale,
Monika E. Polańska, Filip Logist (Eds.)

PSE PRESS

A Century of Data: Thermodynamics and Kinetics for Ammonia Synthesis on Various Commercial Iron-based Catalysts

Hilbert Keestra[a,b,*], Yordi Slotboom[a], Kevin H.R. Rouwenhorst[b,c], Derk W.F. Brilman[a]

[a] Sustainable Process Technology, Faculty of Science and Technology, University of Twente, PO Box 217, 7500 AE Enschede, The Netherlands
[b] Catalytic Processes & Materials, MESA+ Institute for Nanotechnology, University of Twente, PO Box 217, 7500 AE Enschede, the Netherlands
[c] Ammonia Energy Association, 77 Sands Street, 6th Floor, Brooklyn, NY 11201, USA
* Corresponding Author: h.keestra@utwente.nl

ABSTRACT

This work presents an improved thermodynamic model, an equilibrium model, and a unified kinetic model for ammonia synthesis. The thermodynamic model accurately describes the non-ideality of the reaction system up to 1000 bar using a modified Soave-Redlich-Kwong Equation-of-State. The developed Langmuir-Hinshelwood kinetic model accurately describes ammonia synthesis on iron-based catalysts by incorporating N* and H* surface species, whereas H* species are mainly relevant below 400°C. The model fits an extensive dataset across diverse conditions (251-550°C, 1-324 bar, H_2/N_2 ratios 0.33-8.5, and space velocities of 1-1800 Nm^3 kg-cat^{-1} h^{-1}) and accounts for catalyst activity variations through a Relative Catalytic Activity factor.

Keywords: Ammonia, Steady-state kinetics, iron catalyst

INTRODUCTION

Ammonia, with a global demand of 185 Mt in 2020 [1], serves as both a crucial fertilizer component and a promising zero-carbon fuel and hydrogen carrier [2, 3]. Its production via the Haber-Bosch process (Equation 1) relies on iron-based catalysts operating at 350-500°C and 100-300 bar [4]. These catalysts, derived from magnetite (Fe_3O_4) or wüstite ($Fe_{1-x}O$) precursors, incorporate electronic promoters (K_2O) and structural promoters (Al_2O_3, MgO, SiO_2, CaO) to enhance activity and stability [5, 6].

$$3H_2 + 1N_2 \leftrightarrow 2NH_3 \;\; with \;\; \Delta H_r^\circ = -92\ \mathrm{kJ/mol} \qquad (1)$$

While various kinetic models exist for ammonia synthesis [7–10], they are typically based on single-catalyst datasets. This work introduces a comprehensive kinetic model applicable across commercial catalysts at diverse conditions (251-550°C, 1-324 bar), utilizing 11 datasets [7, 8, 10–14] spanning both magnetite and wüstite precursors. The model assumes that despite varying active site densities, the underlying reaction mechanism remains the same across catalysts, with differences in activity addressed through a Relative Catalytic Activity (RCA) correction factor.

Several optimization algorithms were evaluated to fit the kinetic parameters, including Particle Swarm Optimization (PSO), Differential Evolution (DE), Nelder-Mead, compact Genetic Algorithm (cGA), Cobyla, and Powell. The Covariance Matrix Adaptation Evolution Strategy (CMA-ES) proved superior, being the only algorithm to consistently converge to the global minimum across multiple initialization points, likely due to its mechanism to escape local minima in the complex parameter landscape of the kinetic model.

The datasets include various H_2/N_2 ratios and space velocities, making it particularly relevant for renewable ammonia plants with fluctuating hydrogen feedstock. In addition to the kinetic model, a simplified Arrhenius-type equilibrium description is presented for industrial temperature ranges (300-550°C), employing a modified Soave-Redlich-Kwong Equation-of-State with the Mathias alpha function using a polarity correction factor of 0.2368 for ammonia.

THERMODYNAMICS

At high pressures, accurate ammonia synthesis thermodynamics requires an Equation of State (EoS) to account for gas non-ideality [15]. While the Soave-Redlich-Kwong (SRK) EoS is widely used, it poorly describes the polarity of molecules like ammonia at high pressures [16]. This work employs a modified SRK with a polarity correction factor, based on the Mathias alpha function [17], to overcome this limitation.

Existing alternatives to describe the non-ideality, such as Dyson and Simon's polynomials [18] or other EoS [19, 20], lack universal applicability because they are either difficult to implement in commercial flowsheeting software or are inaccurate at high pressures. To address this, a nested fitting method was developed to determine the polarity correction factor in the Mathias alpha function for the SRK EoS. The method was applied to equilibrium data in the range of 300-1100 °C and up to 1000 bar from multiple literature sources.

The resulting equilibrium expression uses a second-order polynomial for reaction enthalpy, simpler than previous higher-order approaches. For practical implementation in software like Aspen HYSYS, we also derived a simplified Arrhenius-type equation valid for 300-550 °C:

$$ln(K_f) = \frac{1}{R}\left(-33.415 - \frac{-4.4401 \cdot 10^4}{T} - 10.578\, ln(T)\right) \quad (2)$$

$$K_f = 1.3632 \cdot 10^{-6} e^{\left(-\frac{-5.1110 \cdot 10^4}{RT}\right)} \quad (3)$$

$$\frac{1}{K_f^2} = 5.3809 \cdot 10^{11} e^{\left(-\frac{1.0222 \cdot 10^5}{RT}\right)} \quad (4)$$

The fitting procedure employs the COBYLA algorithm [21] to optimize the polarity correction factor by minimizing Mean Squared Error, with convergence defined as no improvement beyond the 10th decimal place after 10 iterations.

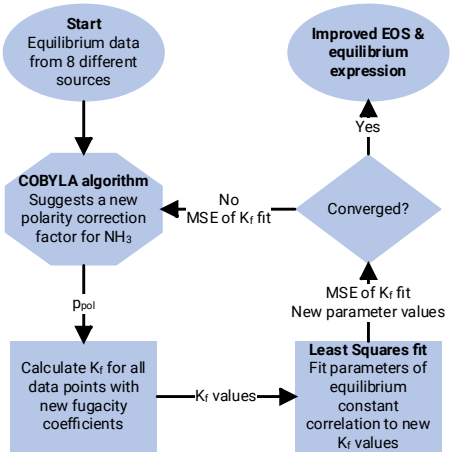

Figure 1. Schematic for the nested fitting method to obtain the polarity correction factor for NH3 and to fit the parameter values of the temperature-dependent equilibrium constant correlations.

The polarity correction factor for NH_3 was fitted to -0.2368 while the polarity factor of the other molecules were kept at zero.

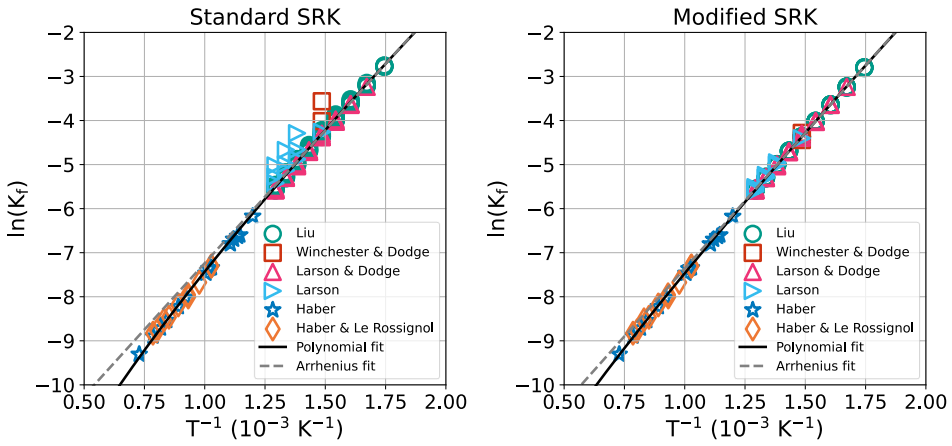

Figure 2: Equilibrium constant prediction by the polynomial (fitted to 300-1100 °C data) and Arrhenius type equation (fitted to 300-550 °C data) without (left) and with (right) polarity correction.

KINETIC MODELLING

Model derivation

The dissociation of surface-adsorbed dinitrogen to atomic nitrogen (Reaction 2 in Table 1) is the rate-determining step for ammonia synthesis on iron-based catalysts [22–24].

Table 1: The microkinetic reactions for ammonia synthesis.

Number	Microkinetic reactions
1	$N_2(g) + * \leftrightarrow N_2*$
2	$N_2* + * \leftrightarrow 2N*$
3	$N* + H* \leftrightarrow NH* + *$
4	$NH* + H* \leftrightarrow NH_2* + *$
5	$NH_2* + H* \leftrightarrow NH_3* + *$
6	$NH_3* \leftrightarrow NH_3(g) + *$
7	$H_2(g) + 2* \leftrightarrow 2H*$

Molecular nitrogen dissociation (reaction 2 in Table 1) was taken as the rate-determining step, and N* and H* were taken as the most abundant surface species on the active sites of the catalyst [25]. A correction factor (b_{cat}) for activity differences between different catalysts was implemented. The derived kinetic model is given in Equation 5,

$$r_{NH_3} = b_{cat} k_{NH_3} f_{N_2} \left(1 - \frac{1}{K_f^2} \frac{f_{NH_3}^2}{f_{N_2} f_{H_2}^3}\right) \left(1 + \frac{f_{NH_3}}{K_N f_{H_2}^{1.5}} + \sqrt{K_H f_{H_2}}\right)^{-2} \quad (5)$$

where f_i stands for the fugacity of a component which is calculated using the modified SRK with the unit bar. K_f is the equilibrium constant calculated using Equation 3. And r_{NH_3} is expressed in mol kg^{-1} s^{-1}. K_N and K_H are adsorption constants for the N* and H* surface species. The adsorption constants and k_{NH_3} follow an Arrhenius relationship and contain, thus, two parameters each.

Modelling procedure

11 datasets found in Refs. [7, 8, 10, 11, 13, 14, 26] with a total of 1019 data points were fitted to the model in Equation 5, over a wide range of temperatures (251-550°C), pressures (1-324 bar), space velocities (1-1800 Nm^3 kg-cat^{-1} h^{-1} at NTP (25 °C and 1 atm)), and H_2/N_2 ratios (0.33-8.5). Only the gas-hour space velocity data were reported for the Fixed Nitrogen No. 660, Temkin & Phyzev, and Fixed Nitrogen Cat. A catalysts. Therefore, the density of those catalysts was assumed to be 3 g cm^{-3}.

The reactor was modelled as an isothermal plug-flow reactor. Due to the wide range of conditions and different orders in magnitude in measured NH_3 molar fractions, a type of normalisation was applied to the objective function. The objective function for the fitting is defined in Equation 6 and 7.

$$\chi^2 = \sum_{j=1} \sigma_j \left(\frac{y_{NH_3,j} - \hat{y}_{NH_3,j}}{y^d_{NH_3,\max}}\right)^2 \quad (6)$$

$$\sigma_j = \frac{1}{N_n} \; with \; j \in N_n \quad (7)$$

Where $y^d_{NH_3,\max}$ is the maximum value of the molar fraction in the dataset. Datasets were equally taken into account by calculating a weight (σ_j) so that the sum of all the weights in a sub-dataset (N_n) was equal to 1. Therefore, there is no bias towards larger datasets.

To improve the predictive capabilities of the model, 5-fold cross-validation was applied. Furthermore, the cross-correlation between parameters was reduced by applying the reference temperature approach by Schwaab et al. [27, 28].

Optimization algorithm selection

Various optimization algorithms were tested to fit the kinetic parameters, including Particle Swarm Optimization (PSO), Differential Evolution (DE), Nelder-Mead, the compact Genetic Algorithm (cGA), COBYLA, and Powell. Among them, the Covariance Matrix Adaptation Evolution Strategy (CMA-ES) with a scale factor of 2.5 demonstrated superior performance, consistently converging to the global minimum across multiple initialization points. This performance is due to its ability to escape local minima in the complex parameter landscape of the kinetic model. The settings for the other algorithms followed the default configurations provided by the Nevergrad [29] optimization package from Meta Inc.

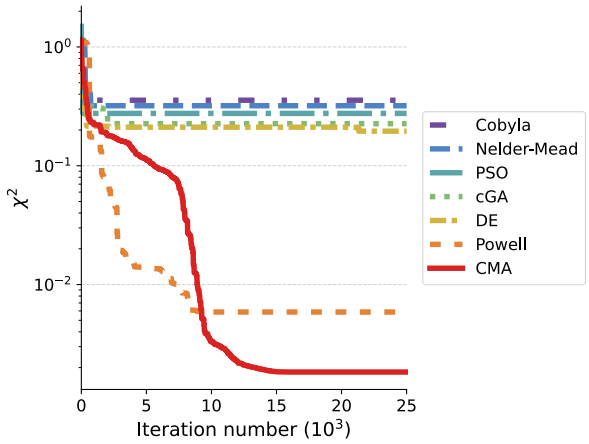

Figure 3. Progression of the optimization algorithms. The displayed error represents the lowest error found up to and including the corresponding iteration number.

Overall fitting results

The calculated parameters for k_{NH_3}, K_N and K_H for the kinetic model are listed in Table 2. And the parameters for the Relative Catalytic Activity factors are found in

Figure 4.

Table 2: Calculated parameters with 95% confidence interval for the kinetic model.

Parameter	Value	± 95% CI	Unit
$k_{NH_3,A}$	2.215E+13	7.624E+13	mol kg-cat^{-1} bar^{-1} s^{-1}
$k_{NH_3,B}$	1.007E+05	7.876E+03	J mol^{-1}
$K_{N,A}$	2.455E-08	6.474E-08	bar$^{-0.5}$
$K_{N,B}$	-1.795E+04	3.365E+03	J mol^{-1}
$\sqrt{K_{H,A}}$	3.276E+02	4.271E+02	bar$^{-0.5}$
$\sqrt{K_{H,B}}$	-4.948E+03	4.887E+03	J mol^{-1}

A parity plot comparing the experimental and predicted NH_3 mole fractions, based on the kinetic model in Equation 5 and the parameters from Table 2, is presented in Figure 4 (Left). This plot incorporates data from 11 datasets featuring different metal oxide precursors, including magnetite and wüstite. The strong agreement between experimental and predicted NH_3 mole fractions supports the hypothesis that all iron-based catalysts reported in literature exhibit similar behavior under operational conditions with respect to temperature and pressure. The primary variations arise from differences in the density of active sites and the effectiveness of promoters, which can be accounted for using a correction factor b_{cat} for catalytic activity.

Multiple models were fitted using the same procedure, and their fitting quality metrics are presented in Table 3. The modified Temkin model, as described by Dyson and Simon [18], features the fewest parameters but exhibits the lowest fit quality, making it more suitable for a narrow operating range. When the model in Equation 5 assumes only N* species, it closely aligns with the model proposed by Nielsen et al. [7]. Substituting partial pressures for fugacities, as implemented by Sehested et al. [8], reduces the fit quality by approximately 20%.

Table 3: Statistical results for the fitted models.

Model	Surface species	MSE	χ^2
Temkin (modified)	-	2.55E-04	3.75E-03
This work	N	1.27E-04	1.67E-03
This work (partial pressure)	N, H	4.83E-05	7.77E-04
This work	N, H	4.05E-05	6.11E-04

CONCLUSION

The modified Soave-Redlich-Kwong Equation-of-State, incorporating a polarity correction factor of -0.2368 for NH_3, effectively accounts for polarity effects at high pressure and accurately describes equilibrium up to 1000 bar. The developed Arrhenius-type equilibrium model and the unified Langmuir-Hinshelwood kinetic model are easily implemented in all commercial flowsheeting software.

The kinetic model successfully describes all available data using a single rate expression and a Relative Catalytic Activity factor per catalyst, capturing variations in active site density and promoter effects. This suggests that ammonia synthesis follows a highly similar mechanism for all iron-based catalysts, regardless of precursor, promoter, or preparation method. The model accurately predicts ammonia synthesis across a broad range of

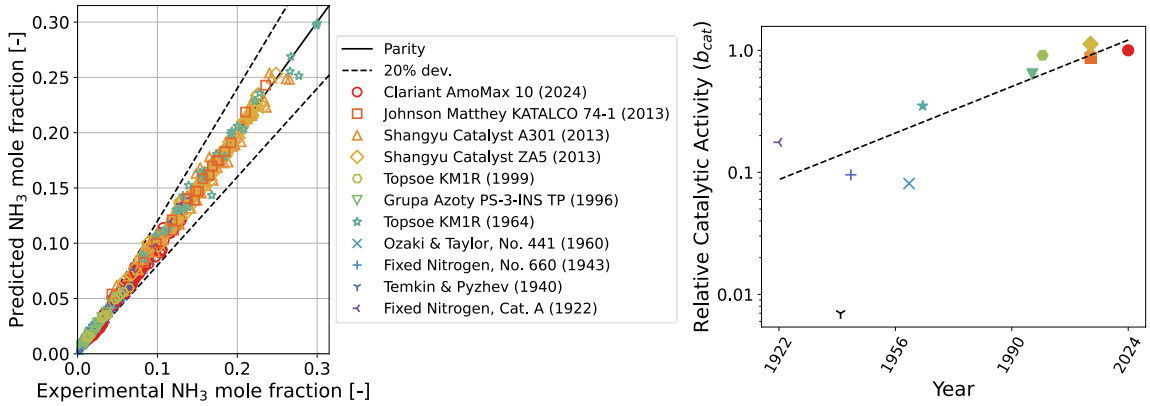

Figure 4: Left: Parity plot of the experimental NH_3 mole fraction in the outlet from Refs. [7, 8, 10, 11, 13, 14, 26] versus predicted NH_3 mole fraction for the same conditions using the model in Equation 5. Right: The calculated Relative Catalytic Activity (b_{cat}) for various datasets. The regression line excludes the Temkin & Pyzhev catalyst because this was the only non-promoted iron catalyst.

conditions (251–550 °C, 1–324 bar, H_2/N_2 ratios of 0.33–8.5, and space velocities of 1–1800 Nm^3 $kg\text{-}cat^{-1}$ h^{-1}). The inclusion of H* surface species are necessary to extrapolate to lower temperatures (<400 °C).

To optimize kinetic parameters, various algorithms were tested, with CMA-ES outperforming others by consistently converging to the global minimum due to its ability to escape local minima in the complex parameter landscape.

This work consolidates over a century of equilibrium and kinetic data for ammonia synthesis using iron-based catalysts with improved and more robust thermodynamic and kinetic models.

ACKNOWLEDGEMENTS

The authors thank the PROVE-IT consortium (RVO MOOI42014) for providing the financial grants for this research. The authors thank Aayan Banerjee, Jimmy Faria, Leon Lefferts, and Sascha Kersten from the University of Twente for the valuable discussions. Furthermore, Tim van Schagen is thanked for their input on the modeling framework.

REFERENCES

1. IRENA, Ammonia Energy Association (2022) Innovation Outlook: Renewable Ammonia. https://doi.org/978-92-9260-423-3
2. Rouwenhorst KHR, Van Der Ham AGJ, Mul G, Kersten SRA (2019) Islanded ammonia power systems: Technology review & conceptual process design. Renewable and Sustainable Energy Reviews. https://doi.org/10.1016/j.rser.2019.109339
3. IRENA (2021) Innovation Outlook: Renewable Methanol.
4. Liu H (2014) Ammonia synthesis catalyst 100 years: Practice, enlightenment and challenge. Cuihua Xuebao/Chinese Journal of Catalysis 35:1619–1640
5. Nielsen A (1995) Ammonia: Catalysis and Manufacture, 1st ed. Springer-Verlag, Berlin Heidelberg
6. Liu H, Han W (2017) Wüstite-based catalyst for ammonia synthesis : Structure , property and performance. Catal Today 297:276–291
7. Nielsen A, Kjaer J, Hansen B (1964) Rate equation and mechanism of ammonia synthesis at industrial conditions. J Catal 3:68–79
8. Sehested J, Jacobsen CJH, Törnqvist E, Rokni S, Stoltze P (1999) Ammonia Synthesis over a Multipromoted Iron Catalyst: Extended Set of Activity Measurements, Microkinetic Model, and Hydrogen Inhibition. J Catal. https://doi.org/10.1006/jcat.1999.2628
9. Temkin M, Pyzhev V (1940) Kinetic of Ammonia Synthesis on Promoted Iron Catalysts. Acta Physicochimica URSS 12:327–356
10. Ozaki A, Taylor H, Boudart M (1960) Kinetics and Mechanism of the Ammonia Synthesis. Proceedings of the Royal Society A: Mathematical, Physical and Engineering Sciences 258:47–62
11. Liu H (2013) Ammonia Synthesis Catalysts: Innovation and Practice. https://doi.org/10.1142/8199
12. Aparicio LM, Dumesic JA (1994) Ammonia synthesis kinetics: Surface chemistry, rate expressions, and kinetic analysis. Top Catal. https://doi.org/10.1007/BF01492278
13. Cholewa T, Steinbach B, Heim C, Nestler F, Nanba T, Güttel R, Salem O (2024) Reaction kinetics for ammonia synthesis using ruthenium and iron based catalysts under low temperature and pressure conditions. Sustain Energy Fuels 8:2245–2255
14. Emmett PH, Kummer JT (1943) Kinetics of Ammonia Synthesis. Ind Eng Chem 35:677–683
15. Soave G (1972) Equilibrium constants from a modified Redlich-Kwong equation of state. Chem Eng Sci 27:1197–1203
16. Graboski MS, Daubert TE (1979) A Modified Soave Equation of State for Phase Equilibrium Calculations. 3. Systems Containing Hydrogen. Industrial and Engineering Chemistry Process Design and Development 18:300–306
17. Mathias PM (1983) A Versatile Phase Equilibrium Equation of State. Industrial and Engineering Chemistry Process Design and Development 22:385–391
18. Dyson DC, Simon JM (1968) Kinetic Expression with Diffusion Correction for Ammonia Synthesis on Industrial Catalyst. Industrial & Engineering Chemistry Fundamentals 7:605–610
19. Beattie JA, Bridgeman OC (1928) A New Equation of State for Fluids. Proceedings of the American Academy of Arts and Sciences 63:229
20. Peng DY, Robinson DB (1976) A New Two-Constant Equation of State. Industrial and Engineering Chemistry Fundamentals 15:59–64
21. Powell MJD (1994) A Direct Search Optimization Method That Models the Objective and Constraint Functions by Linear Interpolation. Advances in Optimization and Numerical Analysis 51–67
22. Aika K-I (2017) Role of alkali promoter in ammonia synthesis over ruthenium catalysts—Effect on reaction mechanism. Catal Today 286:14–20
23. Mortensen JJ, Hansen LB, Hammer B, Nørskov JK (1999) Nitrogen Adsorption and Dissociation on Fe(111). J Catal 182:479–488
24. Ertl G, Lee SB, Weiss M (1982) Adsorption of nitrogen on potassium promoted Fe(111) and (100) surfaces. Surf Sci 114:527–545

25. Sehested J, Jacobsen CJH, Törnqvist E, Rokni S, Stoltze P (1999) Ammonia Synthesis over a Multipromoted Iron Catalyst: Extended Set of Activity Measurements, Microkinetic Model, and Hydrogen Inhibition. J Catal 188:83–89
26. Kowalczyk Z (1996) Effect of potassium on the high pressure kinetics of ammonia synthesis over fused iron catalyst. Catal Letters 37:173–179
27. Schwaab M, Pinto JC (2007) Optimum reference temperature for reparameterization of the Arrhenius equation. Part 1: Problems involving one kinetic constant. Chem Eng Sci 62:2750–2764
28. Schwaab M, Lemos LP, Pinto JC (2008) Optimum reference temperature for reparameterization of the Arrhenius equation. Part 2: Problems involving multiple reparameterizations. Chem Eng Sci 63:2895–2906
29. Bennet P, Doerr C, Moreau A, Rapin J, Teytaud F, Teytaud O (2021) Nevergrad. ACM SIGEVOlution 14:8–15